High-Frequency Green's Function for a Rectangular Array of Dipoles with Weakly Varying Tapered Excitation

F. Mariottini[1], F. Capolino[1], S. Maci[1], and L. B. Felsen[2]

1) Dip. Ingegneria dell'Informazione, Universitá di Siena, Via Roma 56, 53100 Siena, Italy.
2) Dept. Aerospace and Mechanical Eng., and Dept. of Electrical and Comp. Eng., Boston University, 110 Cummington St., Boston, MA 02215, USA.

I. INTRODUCTION

The array Green's function (AGF) is the basic building block for the full-wave analysis of planar phased array antennas. Its representation in terms of element-by-element summation over the individual dipole radiations can be replaced by a more efficient global representation constructed via Poisson summation. The resulting Poisson-transformed integrals can be interpreted as the radiation from continuous equivalent Floquet wave (FW)-matched source distributions extending over the array aperture [1], [2]. Applying high-frequency asymptotics to each FW-matched array aperture casts the AGF in the format of a generalized Geometrical Theory of Diffraction (GTD) which includes conical wavefront edge diffracted rays as well as spherical wavefront vertex diffracted rays. In this paper, the results in [1], valid for equiamplitude excitation, are extended to accommodate tapered illumination, which also includes dipole amplitudes tending to zero at the edges. This extension, which has been performed in [3] with a numerical technique based on the discrete Fourier transform (DFT), is herein carried out by a direct Poisson-transformed asymptotic evaluation of the strip-array GF, with inclusion of asymptotically subdominant "slope" edge and vertex diffracted fields, in addition to the dominant edge and vertex diffracted fields for appreciable edge illumination. Numerical results are presented for illustration.

II. FORMULATION

Consider a rectangular periodic array of $N_1 \times N_2$ linearly phased dipoles located in the z_1, z_2-plane (Fig.1a), with interelement spatial period along the z_1 and z_2 directions given by d_1 and d_2, and the interelement phase gradient by γ_1 and γ_2, respectively. All dipoles are oriented along the unit vector $\hat{\mathbf{J}}_0$ (a bold character denotes a vector quantity, and a caret $\hat{}$ denotes a unit vector). Superimposed upon that background is a z-dependent amplitude-separable tapering function $f(z_1, z_2) = f_1(z_1)f_2(z_2)$, sampled at the dipole locations, $J(n_1 d_1, n_2 d_2) = f_1(n_1 d_1) f_2(n_2 d_2) \exp(-j(\gamma_1 n_1 d_1 + \gamma_2 n_2 d_2))$, with $J(z_1', z_2')$ denoting the dipole current amplitude, and $(z_1', z_2') = (n_1 d_1, n_2 d_2)$ denoting the location of (n_1, n_2)th dipole. A time dependence $\exp(j\omega t)$ is suppressed. Without compromising practical utility, we assume $f(z_1, z_2)$ real and positive in the domain $z_1 \in [0, L_1]$, $z_2 \in [0, L_2]$ and zero elsewhere; here, $L_1 = (N_1 - 1)d_1$ and $L_2 = (N_2 - 1)d_2$. The electromagnetic vector field at any observation point $\mathbf{r} = z_1\hat{\mathbf{z}}_1 + z_2\hat{\mathbf{z}}_2 + y\hat{\mathbf{y}}$ can be derived from the vector potential $\mathbf{A}(\mathbf{r}) = \hat{\mathbf{J}}_0 A(\mathbf{r})$ by summing over the individual (n_1, n_2) dipole radiations $f_1(n_1 d_1) f_2(n_2 d_2) e^{-j(\gamma_1 n_1 d_1 + \gamma_2 n_2 d_2)} \exp(-jkR_{n_1 n_2})/(4\pi R_{n_1 n_2})$ where, $R_{n_1 n_2} = |\mathbf{r} - n_1 d_1 \hat{\mathbf{z}}_1 - n_2 d_2 \hat{\mathbf{z}}_2|$. Employing the (k_{z1}, k_{z2}) spectral Fourier representation of the free space Green's function as shown in [1], yields

$$A(\mathbf{r}) = \frac{1}{8\pi^2 j} \int_{-\infty}^{\infty} \int_{-\infty}^{\infty} I_1(k_{z1}) I_2(k_{z2}) \frac{e^{-jg(k_{z1}, k_{z2})}}{k_y} dk_{z1} dk_{z2}, \tag{1}$$

with $I_i(k_{zi}) = \sum_{n_i=0}^{N_i-1} e^{j(k_{zi} - \gamma_i) n_i d_i} f_i(n_i d_i)$, $i = 1, 2$, $g(k_{z1}, k_{z2}) = k_{z1} z_1 + k_{z2} z_2 + k_y y$ and $k_y = \sqrt{k^2 - k_{z1}^2 - k_{z2}^2}$, with $\Im m\, k_y < 0$ for $k^2 - k_{z2}^2 < k_{z1}^2$, $\Im m\, k_y > 0$ for $k^2 - k_{z2}^2 > k_{z1}^2$ on the top Riemann sheet of the k_{zi}-plane (see [2]). The n_i-sum $I_i(k_{zi})$ in (1) is manipulated via the truncated Poisson sum formula into a (p, q)-sum of Fourier transformed functions $\tilde{f}_i(k_{zi}') = \int_0^{L_i} e^{jz_i k_{zi}'} f_i(z_i) dz_i$, translated by the FW

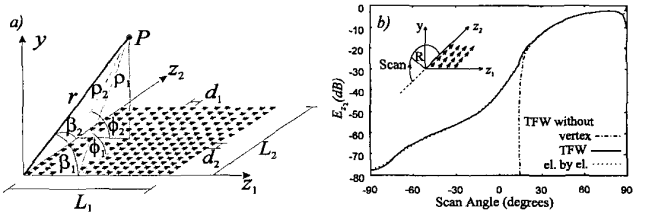

Fig. 1. (a)Geometry of the rectangular array, $\rho_1 = \sqrt{y^2 + z_2^2}$, $\rho_2 = \sqrt{y^2 + z_1^2}$. (b)$E_{z2}$ component of the electric field radiated by a rectangular array with excitation function $f(z_1, z_2) = \prod_i \sin(\pi z_i / L_i)$, at a distance $R = 10\lambda$ from the vertex.

wavenumbers $k_{ziu} = \gamma_i + 2\pi u/d_i$, with $i = 1, 2$ and $u = q, p$; i.e.

$$I_i(k_{zi}) = \frac{f_i(0)}{2} + \frac{f_i(L_i)}{2} e^{j(k_{zi} - \gamma_i)L_i} + \frac{1}{d_i} \sum_{u=-\infty}^{\infty} \tilde{f}(k_{zi} - k_{ziu}). \tag{2}$$

III. HIGH-FREQUENCY SOLUTION

Henceforth, we assume (legitimately for actual tapering functions for large arrays) that $f_i(z_i)$ varies slowly with respect to the wavelength λ. For such weak variation, and since $f_i(z_i)$ is positive in the domain $z_i \in (0, L_i)$, its spectrum $\tilde{f}_i(k'_{zi})$ is localized around $k'_{zi} = 0$, thereby enhancing contributions to $I_i(k_{zi})$ from $k_{zi} = k_{ziu}$. Thus, adiabatic methods can be applied, based on perturbation about $f_i(z_i) = const.$. Consequently, the integral in (1) which defines A is dominated asymptotically by: a) one (k_{z1}, k_{z2}) saddle-point (k^s_{z1}, k^s_{z2}) that satisfies $(d/dk_{zi})g(k_{z1}, k_{z2}) = 0$, yielding the vertex diffracted field; b)"quasi poles" at $k_{zi} = k_{ziu}$ that describe the same phenomenology and localization property as the spectral poles for the semi-infinite array [1], yielding FWs; c)critical points at k^s_{z1} and k^s_{z2} which annul $(d/dk_{z1})g(k_{z1}, k_{z2p})$ and $(d/dk_{z2})g(k_{z1q}, k_{z2})$ respectively, and lead to diffracted fields from edge 2 (located at $z_1 = 0$) and edge 1 (at $z_2 = 0$), respectively. Diffraction from the other two edges can be found similarly by including the appropriate phase reference in the second term in the right side of (2).

Floquet Wave Contributions. Inserting (2) into (1), the contributions due to the critical points at $(k_{z1}, k_{z2}) = (k_{z1q}, k_{z2p})$ are found by expanding the exponent of the integrand in Taylor series in a neighborhood of (k_{z1q}, k_{z2p}) (see [4]). Retaining only the dominant asymptotic term of the remainder which applies for observation points away from the array surface one finals

$$A'(\mathbf{r}) \sim \sum_{p,q} A^{FW}_{pq} f(z_{1pq}, z_{2pq}) \bar{U}_{pq} + ..., \quad A^{FW}_{pq} = \frac{e^{-j(k_{z1q}z_1 + k_{z2p}z_2 + k_{ypq}y)}}{2jd_1 d_2 k_{ypq}}, \tag{3}$$

where $z_{ipq} = z_i - yk_{ziu}/k_{ypq}$, and $k_{ypq} = \sqrt{k^2 - k^2_{z1q} - k^2_{z2p}}$ (with branches chosen according to (1)) is real for propagating FW, and $\bar{U}_{pq} = U(z_{1pq})U(z_{2pq})U(L_1 - z_{1pq})U(L_2 - z_{2pq})$ with $U(z) = 1$ or 0 if $z > 0$ or $z < 0$ respectively. Criteria for the asymptotic validity of the expansion obtained in (3) will be given elsewhere. In (3), A^{FW}_{pq} is the pqth FW for equiamplitude excitation [1], which is multiplied in (3) by the tapering function $f(z_{1pq}, z_{2pq})$ evaluated at the footprint (z_{1pq}, z_{2pq}) of the pqth FW. The stationary phase evaluation of the radiation integral associated with each p, qth equivalent FW-matched aperture distribution would provide the same result

(see 2D case in [5])since (z_{1pq}, z_{2pq}) is the stationary phase point of the p,qth spatial radiation integral. The function U_{pq} is unity or zero for (z_{1pq}, z_{2pq}) is inside or outside the finite array dimensions. The discontinuity of the truncated FW at the Shadow boundary (SB) plane angle defined by $z_{ipq} = 0$ is restored by the diffracted field that arises from the saddle point evaluation of (1).

FW-Induced diffracted contributions. Here, we show only the final result, derived asymptotically in [4], for the diffracted field arising from the truncation at $z_1 \in [0, L_1]$ (edge 1) associated with the critical spectral points $(\bar{k}^s_{z1,q}, k^s_{z2})$. The *total* propagating diffracted field arising from edge 1 is thus represented as $A^{d,1} = \sum_q A^{d,1}_q U^0_q U^{L_1}_q$ where

$$A^{d,1}_q(\mathbf{r}) \sim \frac{e^{-j(k_{z1,q}z_1 + k_{\rho_{1,q}}\rho_1)}}{2d_1\sqrt{2\pi j k_{\rho_{1,q}}\rho_1}} f_1(z^d_{1q}) \left[f_2(0)B_2(\bar{k}^s_{z2})F(\delta^2_{1,pq}) - j f'_2(0)B'_2(\bar{k}^s_{z2})F_s(\delta^2_{1,pq}) \right] \quad (4)$$

in which B_2 and its derivative $B'_2(k_{z2})$ are defined in the text after (5), $F(x)$ is the standard UTD transition function, $F_s(x) = 2jx[1 - F(x)]$ is the slope UTD transition function with argument $\delta^2_{1,pq}$ (defined in [4]) which vanishes at the SB planes, and $U^0_q = U(\beta^{SB}_{1,q} - \beta_1)$, where β_1 is the observation angle (see Fig.1a) (similarly for $U^{L_1}_q$). $A^{d,1}_q$ is the q-th conical wave decaying along ρ_1 and $\beta^{SB}_{1,q} = \beta_1 = \cos^{-1}(k_{z1,q}/k)$ locates the shadow boundary cone (SBC) centered at the vertex, which truncates the domain of existence of the z_1-edge diffracted waves. In (4) the tapering function f_1 is evaluated at the diffraction points $z^d_{1q} = z_1 - y k_{z1,q}/k^s_{yq}$ with $k^s_{yq} = \sqrt{k^2_{\rho 1,q} - (k^s_{z2})^2}$. The discontinuity across the SBC of the edge-diffracted contribution is repaired by the diffraction from the vertex (0,0) of the array. Analogous diffracted fields arise from the other edges.

Vertex diffracted contributions. Near the vertex at $(z_1, z_2) = (0, 0)$, for example, the z_1-edge and z_2-edge planar FW-shadow boundaries interact with the vertex-induced conical SBCs with symmetry axes z_1 and z_2, respectively, that arise form the truncation of the corresponding edge diffracted fields. The confluence of these four SBs near the vertex defines the asymptotics pertaining to the vertex diffracted field $A^{v,1}(\mathbf{r})$, obtained by the following steps. First, I_i in the (2) is expanded asymptotically (integrating by parts up to the second order) as

$$I_i(k_{zi}) \sim f_i(0)B_i(k_{zi}) - j f'_i(0)B'_i(k_{zi}) + O((k_{zi} - k_{zi,u})^{-3}), \quad i = 1, 2 \quad (5)$$

where $B_i(k_{zi}) = [1 - e^{j(k_{zi} - \gamma_i)d_i}]^{-1}$ and $B'_i(k_{zi}) = j d_i e^{j(k_{zi} - \gamma_i)d_i}/[1 - e^{j(k_{zi} - \gamma_i)d_i}]^2$ is its derivative. Next, the integration contours are locally deformed along a 45^o-line through the (k^s_{z1}, k^s_{z2}) saddle point and then extended parallel the real axis (see [2]). Thus, inserting in to (1) the two terms of the asymptotic expansion of $I_i(k_{zi})$, $i = 1, 2$, we have $A^{v,1}(\mathbf{r}) \sim \sum_{h=1}^4 A^{v,1}_h(\mathbf{r})$ expressed as a sum of four terms. The asymptotics is then obtained by the Pauly-Clemmow method. Within this method, the asymptotic evaluation of integrals characterized by specific arrangements of critical points (saddle points (SPs) and singularities) is addressed by mapping the given integrand (both phase and amplitude) onto the simplest canonical integrand that accommodates the relevant critical point configuration. For the vertex problem, the critical parameters are tied to the $(k_{z1}, k_{z2}) = (k^s_{z1}, k^s_{z2}) = (k\cos\beta_1, k\cos\beta_2)$ first order SP, and to the k_{z1}- and k_{z2}-poles in (1). For details, see [2]. The final asymptotics for each h-indexed integral yields

$$A^{v,1}_h(\mathbf{r}) \sim \frac{(-1)^{m+l+1} f^{(m)}_1(0) f^{(l)}_2(0)}{4\pi r j^{m+l+2}} e^{-jkr} B^{(m)}_1(\bar{k}^s_{z1}) B^{(l)}_2(\bar{k}^s_{z2}) T_h(a_q, b_p, w) \quad (6)$$

where

$$T_h(a_q, b_p, w) = \frac{a_q^{m+1} b_p^{l+1}}{j\pi c} \int_{-\infty}^{\infty} \int_{-\infty}^{\infty} \frac{e^{j(\xi^2 + 2w\xi\eta + \eta^2)}}{(\xi - \frac{a_q}{\sqrt{1-w^2}})^{m+1} (\eta - \frac{b_p}{\sqrt{1-w^2}})^{l+1}} d\xi d\eta \qquad (7)$$

are the canonical transition functions. In (7), the parameters a_q, b_p and ξ, η are defined in [2], the superscript $^{(\alpha)}$ denotes the α-th derivative and, for $h = 1$, $m = l = 0$, $c = (1 - w^2)^{1/2}$; for $h = 2$, $m = 0$, $l = 1$, $c = -(1 - w^2)$; for $h = 3$, $m = 1$, $l = 0$, $c = -(1 - w^2)$; for $h = 4$, $m = 1$, $l = 1$, $c = (1 - w^2)^{3/2}$. The numerical evaluation of the integrals T_h can be performed in terms of an algebric sum of standard Generalized Fresnel Integrals and UTD transition functions. It is found (see [2]) that the vertex-diffracted contribution $A_1^{v,1}$ containing the integral function T_1 accounts for the transition from a vertex-centered spherical wave to an edge-centered cylindrical wave and it compensates for the discontinuities across the SBCs. The other vertex diffracted terms $A_h^{v,i}$ are of higher asymptotic order and compensate for the discontinuities across the SBCs when the $f_i(z_i)$ is weakly tapered. Note that when the excitation-function tends to zero at the vertex, only the $A_4^{v,i}$ contribution remains.

Numerical Example. The total high frequency solution is

$$A = \sum_{p,q} A_{pq}^{FW} f(z_{1,pq}, z_{2,pq}) \bar{U}_{pq} + \sum_{i=1}^{4} \left(\sum_{u} A_u^{d,i} U_u^0 U_u^L \right) + \sum_{i=1}^{4} \left(\sum_{h=1}^{4} A_h^{v,i} \right) \qquad (8)$$

with $u = q$ for $i = 1, 3$; $u = p$ for $i = 2, 4$. The preliminary numerical example in Fig.1b shows the accuracy of the truncated Floquet wave (TFW) asymptotics in (8), including the transition region close to the SBC_1, when compared with a reference solution obtained by an element-by-element summation over the contributions from each dipole. The test array has $N_1 = N_2 = 200$ elements. The dipoles are oriented along z_2 with interelement spacings $d_1 = d_2 = 0.5\lambda$, interelement phasings $\gamma_1 = \gamma_2 = 1.52/\lambda$ and tapering $f(z_1, z_2) = \prod_i \sin(\pi z_i / L_i)$. Electromagnetic quantities are evaluated from the vector potential as in [1], and only the E_{z_2} component is shown in Fig.1b along a scan at $R = 10\lambda$ in the y, z_2 plane from the vertex of the array. We observe that when the observation point P passes through $\beta_2 = \beta_{2,0}^{SB} = 76^o$ (scan angles= 14^o in Fig.1b), the TFW without the vertex contribution vanishes, and the tip contribution provides the required continuity for the total field. In this particulare case, $f_i(0) = f_i(L_i) = 0$; thus the diffracted field and the vertex field involve only the terms $f_i'(0)$, therefore providing a good test case for the additional "slope edge- and vertex-diffracted fields".

References

[1] F. Capolino, M. Albani, S. Maci, and L.B. Felsen, "Frequency domain Green's function for a planar periodic semi-infinite dipole array. Part I: Truncated Floquet wave formulation," *IEEE Trans. Antennas Propagat.*, vol. 48, no. 1, pp. 67–74, January 2000.

[2] F. Capolino S. Maci and L. B. Felsen, "Asymptotic high-frequency Green's function for a planar phased sectoral array of dipoles," *Radio Science-Invited Paper*, vol. 35, no. 2, pp. 579–593, March-April 2000, Ser. Special Issue 1998 URSI Int. Symp. Electromagn. Theory.

[3] P. Nepa, P.H. Pathak, Ö. A. Çivi, H-T. Chou, "A DFT based UTD ray analysis of the EM radiation from elettrically large antenna arrays with tapered distribution," in *IEEE AP-S/URSI Symposium*, Orlando, FL, July 11-16 1999, p. 85.

[4] F. Capolino, S. Maci and L. B. Felsen, "Floquet wave diffraction theory for tapered planar array Green's function," in *AP2000 Millennium Conf. Ant. Propagat.*, Davos, Switzerland, April 9-14 2000.

[5] L.B. Felsen and L. Carin, "Diffraction theory of frequency- and time-domain scattering by weakly aperiodic truncated thin-wire gratings," *J. Opt. Soc. Am. A*, vol. 11, no. 4, pp. 1291–1306, April 1994.